Pearl Farming Micro-Nanoplastics Affect Oyster Physiology and Pearl Quality

Tony Gardon (tony.gardon@ifremer.fr)
Ifremer
Jérémy Le Luyer
Université Laval https://orcid.org/0000-0001-9409-3196
Gilles Le Moullac
French Research Institute for Exploitation of the Sea
Claude Soyez
Ifremer
Fabienne Lagarde
IMMM
Alexandre Dehaut
ANSES
Ika Paul-Pont
CNRS
Arnaud Huvet
Institut français de recherche pour l'exploitation de la mer https://orcid.org/0000-0001-6912-881X

Research Article

Keywords: Pearl oyster, micro-nanoplastic exposure, environmental scenarios, ecophysiology, energy metabolism, functional genomics, pearl cycle

Posted Date: January 15th, 2024

DOI: https://doi.org/10.21203/rs.3.rs-3127557/v5

Additional Declarations: The authors declare no competing interests.

Pearl Farming Micro-Nanoplastics Affect Oyster Physiology and Pearl Quality

Tony Gardon,[a,*] Jérémy Le Luyer,[a] Gilles Le Moullac,[a] Claude Soyez,[a] Fabienne Lagarde,[b] Alexandre Dehaut,[c] Ika Paul-Pont,[d] and Arnaud Huvet[d]

[a] Ifremer, ILM, IRD, University of French Polynesia, EIO, F-98719, Taravao, Tahiti, French Polynesia, France.

[b] Institute of Molecules and Materials of Le Mans, IMMM – UMR CNRS 6283, University of Le Mans, Avenue Olivier Messiaen, 72085, Le Mans, France.

[c] ANSES – LSA, Boulevard du Bassin Napoléon, 62200, Boulogne-sur-Mer, France.

[d] University of Brest, Ifremer, CNRS, IRD, LEMAR, F-29280, Plouzané, France.

* Corresponding author: Tony Gardon

E-mail: tony.gardon@ifremer.fr; ORCID ID: 0000-0002-5761-0526

Abstract: Pearl farming is crucial for the economy of French Polynesia. However, rearing structures contribute significantly to plastic waste, and the widespread contamination of pearl farming lagoons by microplastics has raised concerns about risks to the pearl industry. This study aimed to evaluate the effects of micro-nanoplastics (MNPs, 0.4–200 µm) on the pearl oyster (*Pinctada margaritifera*) over a 5-month pearl production cycle by closely mimicking ecological scenarios. MNPs were produced from weathered plastic pearl farming gear and tested at environmentally relevant concentrations (0.025 and 1 µg L^{-1}) to decipher biological and functional responses through integrative approaches. The significant findings highlighted impacts of MNPs on oyster physiology and pearl quality, even at remarkably low concentrations. Exposure to MNPs induced changes in energy metabolism, predominantly driven by reduced assimilation efficiency of microalgae, leading to alteration in gene expression patterns. A distinct gene expression module exhibited a strong correlation with physiological parameters affected by MNP conditions, identifying key genes as potential environmental indicators to nutritional-MNP stress in cultured oysters. The alteration in pearl biomineralization, evidenced by thinner aragonite crystals and the presence of abnormal biomineral concretions, known as keshi pearls, raises concerns about the potential long-term impact on the Polynesian pearl industry.

Keywords: *Pearl oyster, micro-nanoplastic exposure, environmental scenarios, ecophysiology, energy metabolism, functional genomics, pearl cycle*

Synopsis: Limited lab research investigates ecologically simulated microplastic exposure. This study reveals micro-nanoplastic conditions that cultivated pearl oysters may encounter in lagoons could jeopardize oyster health and pearl quality, impacting Polynesian industry.

TOC/Abstract graphic

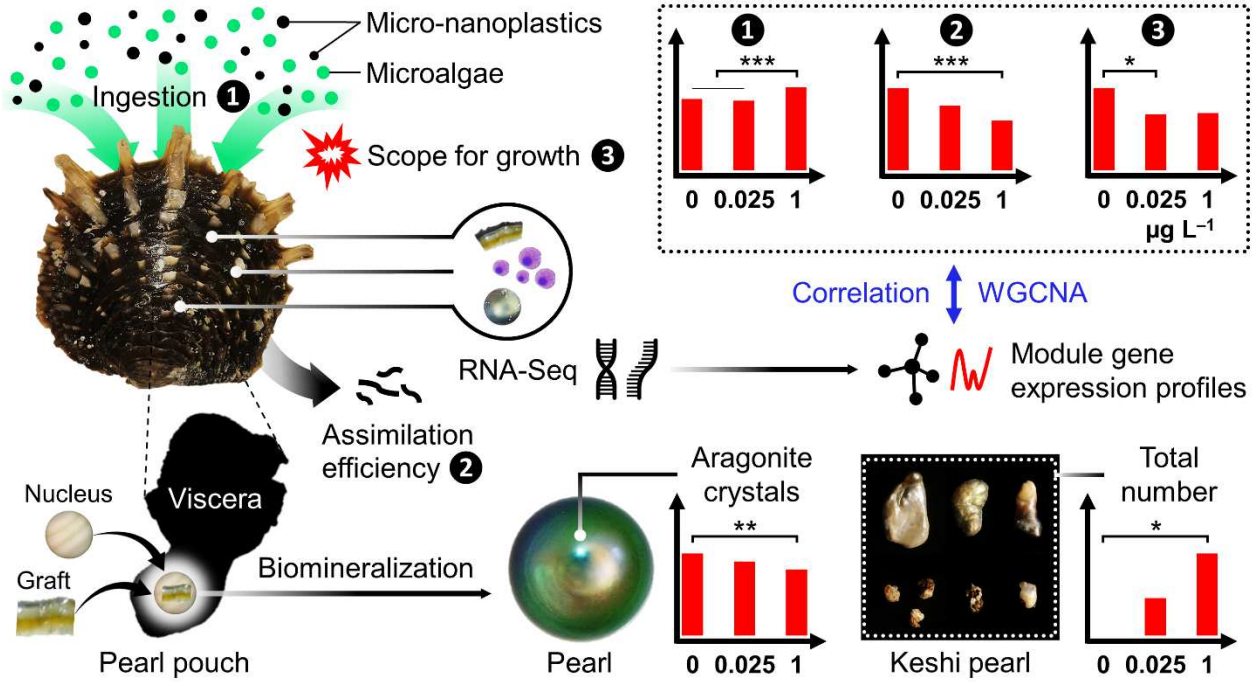

Introduction

Mounting volumes of plastic debris in the environment have become a global concern. With plastic production and consumption surpassing proper waste management capabilities, plastic waste accumulates in the environment, particularly in the ocean.[1] Plastic debris can remain in the marine environment for many years due to slow degradability.[2] Driven by various environmental factors,[3] larger plastic pieces break down into smaller fragments, of which 92% are microplastics (MPs) of 0.33–5 mm in size,[4] excluding consideration for smaller MPs and nanoplastics (NPs, <0.1 μm) that are as yet poorly quantified in nature.[5] Given their pervasive presence and small size, MPs have emerged as a worldwide issue, intensifying concerns about their ecological impacts.[6] MPs are prone to ingestion by a diverse range of organisms,[7] as evidenced by laboratory experiments on

filter-feeding species,[8,9] and by the presence of MPs in the digestive tracts of wild animals.[10,11] Experimental consumption of MP can lead to detrimental health effects, affecting functions such as respiration,[12] nutrition,[13] assimilation efficiency,[9] reproduction,[8] and growth.[14] Yet, most laboratory experiments have utilized single polymer type, usually spherical in shape (termed model particles), often at higher concentrations in terms of particle count per volume than real-world settings.[15,16] Although this type of study is necessary to understand the toxicity mechanisms at play,[17] it lacks ecological relevance regarding the real environmental MP exposure complexity, encompassing diverse particle shapes, sizes, polymer types, surface characteristics, chemical properties, and biological load, underscoring the challenges of investigating the actual ecological impact of MPs in aquatic ecosystems.[16,17] While, a handful of studies have tried to consider the complexity of *in situ* MP exposure,[18–20] a significant disparity persists between potential risks and actual risks associated with MPs,[16,21] largely due to limitations in replicating these conditions in laboratory settings.

In French Polynesia (FP), pearl farming ranks as the second most important economic resource, contributing to $22.3 million in 2020. The trade of pearls and mother-of-pearl is widespread across 28 island and atoll lagoons.[22] Nonetheless, pearl farming is linked to a distinct plastic source, as much of the equipment (*e.g.*, ropes, collectors, and buoys) is fashioned from synthetic materials that accumulate over time, potentially becoming sites for the release of MPs.[23] Recent monitoring in pearl farming lagoons revealed extensive MP contamination in both the seawater and cultured oysters.[24] The water column, a vital environment for cultivating pearl oysters (*Pinctada margaritifera*), emerged as a heavily contaminated compartment (14–716 MP m^{-3}); this means that *P. margaritifera* is exposed to substantial microscale MP pollution (2–125 MP g^{-1} dry weight).[24] Ropes and spat collectors—key plastic components in pearl farming, constructed from polyethylene (PE) and polypropylene (PP)—were identified as major contributors to the abundance

of small-sized (20–200 µm) and fragment-shaped MPs.[24] Consequently, pearl farming could inadvertently contribute to its own plastic pollution risk, potentially affecting pearl oysters and leading to broader repercussions on marine life and lagoon ecosystems.

Experimental exposure to polystyrene microbeads has already shown a dose-dependent (0.25, 2.5, and 25 µg L^{-1}) effect on energy balance,[9] and dose-specific transcriptomic disruption of gene expression[25] in *P. margaritifera*. In this study, we simulated more realistic scenarios by exposing pearl oysters to micro-nanoplastics (MNPs) from pearl farming equipment over a 5-month pearl production cycle. Three MNP concentrations were tested: 0 (control), 0.025, and 1 µg L^{-1}. We employed integrative approaches to assess the impacts of this exposure at individual, cellular, and molecular levels, while also evaluating crucial endpoints such as pearl quality. Demonstrating effects in a more realistic context aims to inform decision-making, stimulate changes in industry processes, and influence legislation by outlining government policies to mitigate this emerging risk to lagoon ecosystems and the sustainability of pearl farming.

Materials and Methods

Experimental animals. Pearl oysters were sampled on April 03, 2018, in a pearl farm located on Mangareva Island (23°06′34″S; 134°57′57″W) in the Gambier archipelago (23°07′S; 134°58′W, FP). A stock of 600 adult oysters (1.5–2 years old) was transferred (transfer authorization No. 643 issued by the Ministry of Marine Resources of FP) to the lagoon of Vairao (Ifremer marine concession No. 8120/MLD: 17°48′26.0″S, 149°18′14.4″W, Tahiti, FP) on April 04, 2018. All the experimental procedures comply with French law and with institutional guidelines.

Pearl farming MNPs. MNPs were produced from two widely used types of pearl farming plastic gear (*i.e.*, synthetic rope and spat collectors), collected from weathered structures of a pearl farm in Manihi atoll (14°24′10.4″S, 145°57′29.2″W), according to the methodological protocol of Gardon et al.[26] Based on FTIR and Py-GC-MS measurements, the synthetic rope (SR) and spat collector (SC) were made of PE and PP, respectively (Figure S1). These two polymers are the most commonly used plastic polymers worldwide and are often found in MPs sampled from pearl farming atolls.[24] The MNP size distribution ranged from 0.4 to 200 µm (Figure S2) following laser diffraction analysis (Beckman Coulter LS 130 particle laser diffractometer, Beckman Coulter, Inc., Brea, CA), matching the retention size range of *P. margaritifera* (*i.e.*, 2–200 µm).[27] MNPs produced from SR and SC were conserved separately in stock solutions, resuspended in filtered (1.2 µm) 70% ethanol at 1.5 g L^{-1} and stored at 4 °C.

MNP exposure. A total of 240 pearl oysters (height, 7.6 ± 0.3 cm; weight, 36.1 ± 5.5 g) were conditioned in duplicate in 6 rectangular 500 L tanks (4 donors and 36 receivers for a total of 40 pearl oysters per tank, 80 oysters per condition) supplied by natural seawater directly pumped and filtered (25 and 5 µm) from the lagoon at 26.5 ± 0.6 °C (pH 8.2, dissolved oxygen 6.8 ± 0.5 mg O_2 L^{-1}, salinity 35 psu), and kept under a 12 h light: 12 h dark cycle. The tanks were equipped with 2 air-lifts connected to the pressurized air circuit and 4 circulation pumps in order to maintain a homogeneous environment around the oysters. A mixed diet of two microalgae (*Tisochrysis lutea* [*T-iso*] and *Chaetoceros gracilis*), used as optimal food for *P. margaritifera* in laboratory settings,[27,28] was continuously supplied at a dry-weight-algae/dry-weight-oyster ratio of 7–8% (*i.e.*, 35–40 cells μl^{-1}, below the threshold for triggering pseudofeces production). Before exposure, pearl oysters were placed in a 500 L tank for calcein marking performed at 150 mg L^{-1} (calcein diluted in seawater) overnight to assess the shell growth rate (refer to the Supporting Information).[29]

After 2 weeks of acclimation, both types of MNPs (*i.e.*, SR and SC) were incorporated at equal weights (ratio SC/SR = ~5.2) and injected continuously at concentrations of 0 (control), 0.025 and 1 µg L^{-1}. The MNP concentrations tested in the present study were similar in terms of MP mass concentration to estimates from Gardon et al.[24] of concentrations that may occur in the pearl oyster living environment. The tested mass concentrations of 0.025 and 1 µg L^{-1} are both included within the range of 0.003–3 µg L^{-1} (for particle size ranging from 20 to 200 µm) extrapolated from *in situ* data points of 716 MP m^{-3} measured in the water column of the pearl farming atoll of Takaroa.[24] Here, we tested 0.4–200 µm MNPs at 0.025 µg L^{-1} (~2.8×10^{6} MNPs L^{-1}) in order to target a response window where no effect occur for MNP stress based on previously reported dose-effects (0.25, 2.5, and 25 µg L^{-1}) on oyster physiology,[9] and gene expression.[25] Thus, we reduced the previously lowest tested dose of 0.25 µg L^{-1} by a factor of 10 to achieve 0.025 µg L^{-1}. A 40-fold higher dose of 1 µg L^{-1} (~1.1×10^{8} MNPs L^{-1}) was also tested in order to overlap with previous tested concentrations and match the linear regression of extrapolated field data suggested by Lenz et al. (2016).[16] These two concentrations were therefore tested to get as close as possible to the "current" scenario (*i.e.*, number of particles per volume *vs.* mass concentration). The MNP mixture was incorporated in 5 µm-filtered seawater and distributed continuously from a solution prepared daily in six cylindrical-conical 50 L tanks (1 per replicate). To limit aggregation, MNP solutions were added with Tween® 20 at a final concentration of 0.0002% (which is below the nontoxic concentration, 0.0007% v/v),[30] and distributed in all tanks, including the control. Due to methodological limitations in detecting and accurately quantifying polydisperse MNPs (with 80-90% of particles <1 µm, Figure S2) in exposure media, especially at such low concentrations, adjustments in concentrations were made based on previous research. This research highlighted disparities between expected and actual concentrations in experimental tanks, indicating an exposure 13-15% lower than the theoretically distributed concentrations.[8,9] Consequently, an

exposure level 13% higher than the theoretical levels was implemented to compensate for particle loss and biomass-induced variations within the experimental design.

Experimental grafts. After 2 months of exposure, pearl oysters were removed from the water for processing for the graft step. Receiver oysters were half-opened with a prop, and donor oysters were sacrificed. Ten mantle grafts from each donor were sampled and transplanted to receivers (1 donor for 10 receivers). For each receiver, one graft and one nucleus (2.0 BU size, Ø ~0.6 mm, ~0.4 g weight; Imai Seikaku Co. Ltd., Japan) were both inserted into the pearl pouch by a transplant specialist to simulate a pearl production cycle. Each nucleus was previously weighed with a highly accurate balance with ± 0.0001 mg accuracy to assess pearl nacre deposition on the surface after harvesting at the end of the exposure. One nucleus transplanted to one of the 10 receivers per donor was a magnetized nucleus (*i.e.*, 4 per tank, 8 per treatment) for the assessment of pearl rotation in the pearl pouch (see Supporting Information).[31,32] Once the receivers were grafted, all pearl oysters were put back in their respective experimental tanks to continue MNP exposure over a 3-month period.

Ecophysiological measurement. At 2 weeks post-graft (2.5 months exposure), ten receiver oysters per treatment were placed individually in an ecophysiological measurement system (EMS) to monitor the clearance rate (ingestion) and oxygen consumption. Details of the EMS acquisition system are provided in the Supporting Information. Assimilation efficiency was measured after collecting feces in each hemispheric chamber and 50 ml of microalgae mixture administered during ecophysiological measurements.[33] Ecophysiological measurements were conducted during the 2.5- to 4-month exposure period, with each condition alternated between each run of 48-h data acquisition. A total of 120 pearl oysters were individually monitored in the EMS, with 40 oysters per treatment. After each run, the oysters were returned to their original experimental tank to

continue exposure until the end of the 5-month experiment, during which RNA-Seq and pearl quality analyses were conducted on the same individuals to explore potential connections.

Metabolic rates including ingestion, oxygen consumption, and assimilation efficiency, used to calculate the scope for growth (SFG), were computed following Chávez-Villalba et al.,[33] and describe in Gardon et al.[9] Detailed calculations are provided in the Supporting Information as Supplementary Methods.

Oyster sampling. Pearl products were collected at the end of the 5-month exposure period. Measurements of pearl quality traits were conducted on biomineral structures formed around the nucleus, with a specific emphasis on the microstructures of aragonite crystals (see Supporting Information). Keshi pearl production sometimes occurs after nucleus rejection and corresponds to the biomineralization of the remaining grafted piece of mantle and/or particles that may penetrate the pearl pouch before healing of the transplantation incision. An analysis of keshi pearls was carried out to determine the origin of these biomineral concretions, following the procedures outlined by Hermabessiere et al.[34] and Djouina et al.[35] (see Supporting Information). The visceral mass was then sampled, drained on absorbent paper and placed in 10% formalin seawater for 72 h before being transferred into 70% ethanol for histology analysis (see Supporting Information). A piece of mantle and a piece of pearl sac (in the case of pearl harvest) were also sampled from each pearl oyster, as well as hemocytes collected in the byssal gland with a needle (1 ml; 0.45 × 13 mm). These samples were placed in RNA later solution (500 µl) and stored at –80 °C for downstream transcriptomics. Each muscle from each pearl oyster was also sampled and frozen in liquid nitrogen before storage at –80 °C for energy reserve assessment by glycogen content (see Supporting Information).

RNA extraction and sequencing. Total RNA was extracted from mantle, hemocyte and pearl sac samples with TRIZOL Reagent (Life Technologies, USA) at a ratio of 1 ml per 100 mg tissue. RNA quantity and integrity were evaluated with a Nanodrop (NanoDrop Technologies Inc., USA) and a 2100 BioAnalyzer System (Agilent Technologies, USA). RNA was dried in RNA-stable solution (Thermo Fisher Scientific, USA) and shipped at ambient temperature to McGill sequencing platform services (Montreal, Canada). TruSeq RNA libraries were randomly multiplexed (N = 20 individuals per lane) and subjected to 100-bp paired-end sequencing on an Illumina NovaSeq 6000 system at the McGill Genome Quebec platform (Montreal, CA).

RNA-Seq data analysis. Raw reads were first filtered with Trimmomatic v0.38 with a minimum length (60 bp),[36] minimum quality (leading: 20; trailing: 20), and the presence of putative contaminants and remaining adaptors. Read quality was assessed before and after trimming with FastQC v0.11.8 and MultiQC v1.6.[37] Only high-quality paired-end reads were retained and mapped against the reference genome[38] using GSNAP v2018.07.04 with default parameters[39] but allowing a minimum mismatch value of 2 and a minimum read coverage of 90%. We used only properly paired and uniquely mapped reads for the downstream analysis.[39]

Differential gene expression was assessed through pairwise comparisons and Wald tests using the *DESeq2* v1.22.2 R package.[40] Genes were considered differentially expressed (DEGs) when the absolute value of $\log_2$FC was > 2 and the false discovery rate (FDR) was < 0.01. The *KOGMWU* package[41] was used to test for rank-based enrichment of eukaryotic orthologous groups (KOG) and Gene Ontology (GO) terms using EggNOG-mapper v2.0[42] in the mantle, hemocytes and pearl sac sequencing datasets. The KOG_MWU function calculates delta rank values for these 23 broad functional groups using $\log_2$FC values for the entire datasets. Functional responses to 0.025 and 1 µg L^{-1} MNPs were compared according to sample type to identify common and

divergent patterns. Supplementary comparisons were performed between sample types for each MNP condition to identify common responses among tissue samples.

Weighted gene coexpression network analysis (WGCNA), implemented in R (v4.1.2) and based on variance-stabilization (VST) data values, was used to identify modules of genes in mantle, pearl sac, and hemocytes, whose expression significantly correlated with conditions (control, 0.025, and 1 µg L^{-1}), MNP conditions (0.025 and 1 µg L^{-1}), and physiological and functional traits associated with the same individuals (except for hemocytes, where only 10 common oysters out of 29, representing 3–4 individuals per condition, due to sampling feasibility). A signed network was constructed using a soft threshold power of 13, a minimum module size of 50, and a module merging threshold of 25% dissimilarity. Module–trait relationships were computed by Pearson's correlation tests. Modules exhibiting a $r \geq 0.45$ and $P \leq 0.01$ were selected as modules of interest. Eigengene expression within each module was also statistically tested to identify significant differences between conditions. GO enrichment analysis for biological process (BP) and molecular function (MF) was performed on module genes using the Mann–Whitney *U* test implemented in the GOMWU framework using module kME input file, *P. margaritifera* annotations, *go.obo* database and a custom Perl script.

The Genes in WGCNA modules of interest were then overlapped with DEG list to identify potential links with differences between conditions, as well as associated physiological and functional trait relationships.

Statistical analysis. Data are presented as the mean with the 95% confidence interval of the mean (mean ± 1.96 standard error), except for frequency distributions, where data are presented as the mean ± standard deviation. Normality and homoscedasticity were tested with Shapiro–Wilk and Levene's tests, respectively. Data expressed in relative values were previously transformed by the arcsine square root function. Mean values of a single-response variable were compared using a

one-way ANOVA for the condition factor ($\alpha = 0.05$). Tukey's post hoc test was used to evaluate the significance of differences between the averages of each group. When the assumptions of normality and homogeneity of variance were not met, even after data transformations (square root, logarithmic, and Box-Cox transformations), we used the nonparametric Kruskal–Wallis' (KW) test to compare the means of each condition. Dunn's post hoc test, employing the Bonferroni-adjusted *P*-values, was used for multiple comparisons and to assess the significance of differences between the means of each group. Frequency distributions were analyzed using Pearson's chi-squared test to determine if a difference occurred between conditions. Fisher's exact test was then used to compare conditions using a 2 × 2 contingency table. The results were considered significant at $P \leq 0.05$. All analyses were performed in the statistics software RStudio v4.1.2.

Results

Metabolic rates. MNP exposure led to a significantly higher ingestion rate in oysters exposed to 1 µg L^{-1} (12.4 ± 0.6 × 10^7 cells h^{-1} g^{-1}) than in oysters exposed to the control (10.7 ± 0.5 × 10^7 cells h^{-1} g^{-1}) and 0.025 µg L^{-1} (10.5 ± 0.6 × 10^7 cells h^{-1} g^{-1}) conditions (Tukey's HSD, $P < 0.001$) (Figure 1B). Furthermore, a significantly lower assimilation efficiency was observed in oysters exposed to 1 µg L^{-1} (26.1 ± 5.2%) than in control oysters (37.5 ± 3.4%; Tukey's HSD, $P < 0.001$), while only a downward trend was observed in oysters in the 0.025 µg L^{-1} condition (31.4 ± 3.3%; Tukey's HSD, $P = 0.100$) (Figure 1D). No significant difference was observed regarding oxygen consumption (ANOVA, $P = 0.420$), with a mean of 0.79 ± 0.08, 0.81 ± 0.07 and 0.85 ± 0.06 mg O_2 h^{-1} g^{-1} under control, 0.025 µg L^{-1} and 1 µg L^{-1} conditions, respectively (Figure 1C).

Scope for growth. Metabolic rate analysis revealed a mean energy balance (scope for growth) of 31.2 ± 3.9, 22.2 ± 4.7 and 22.6 ± 6.8 J h^{-1} g^{-1} for the control, 0.025 µg L^{-1} MNP and 1

µg L^{-1} MNP conditions, respectively (Figure 1E). The overall KW test was at the limit of significance ($P = 0.050$), and multiple comparisons revealed a slight significant difference in means between the control and 0.025 µg L^{-1} conditions (Dunn's test, $P = 0.048$) (Figure 1E).

Energy reserve and shell growth. The glycogen content analysis on pearl oyster muscle revealed a significantly lower energy reserve in the 0.025 µg L^{-1} (4.6 ± 0.8 µg mg^{-1}) condition compared with the control (8.1 ± 1.2 µg mg^{-1}) and 1 µg L^{-1} (7.9 ± 1.5 µg mg^{-1}) conditions (Tukey's HSD test, $P < 0.001$ and $P = 0.001$, respectively) (Figure 1F). No significant difference in shell growth was observed among conditions (ANOVA, $P = 0.321$, Figure 1G).

Harvest. The number of pearls collected at the end of the experiment showed statistically similar frequency distribution among conditions ($\chi^2 = 0.164$, $P = 0.921$). The mean percentages were 62.4% ± 12.8% ($N = 23$) for individuals producing pearls in the control condition, 59.7% ± 17.4% ($N = 27$) and 59.9% ± 11.4% ($N = 31$) for those in the 0.025 and 1 µg L^{-1} conditions, respectively (Figure 2A and B). However, a significant difference in the frequency distribution of keshi pearl production, involving pearl oysters that have rejected their nucleus (Figure 2A and C), emerged between the control and 1 µg L^{-1} conditions (Fisher's exact test, $P = 0.039$). The 0.025 µg L^{-1} condition showed an intermediate value that was not significantly different (Fisher's exact test, $P = 0.144$). Specifically, the 0.025 µg L^{-1} condition exhibited a mean of 9.9% ± 8.3% ($N = 4$) and the 1 µg L^{-1} condition showed 17.6% ± 9.1% ($N = 9$) of pearl oysters producing keshi pearls. Conversely, no keshi pearls were collected from the control condition ($N = 0$; Figure 2A).

Pearl quality traits. Pearl nacre deposition measured on the nucleus and composed of periostracum, calcite and aragonite crystals (Figure 2D) reached similar mean values of 80.2 ± 12.2 µg in the control condition, 85.4 ± 17.8 µg in the 0.025 µg L^{-1} condition, and 78.0 ± 21.1 µg in the 1 µg L^{-1} condition (KW test, $P = 0.717$). Similarly, no significant difference in biomineralization rate (thickness) was measured among conditions (ANOVA, $P = 0.430$), with values of 3.0 ± 0.5,

3.4 ± 0.7 and 2.9 ± 0.6 µm d^{-1} in the control, 0.025 and 1 µg L^{-1} conditions, respectively (Figure 2E). However, a significantly higher proportion of organic material in the coating on the nucleus (periostracum) was measured in the 0.025 µg L^{-1} condition (7.3 ± 6.5%) compared to the control (1.2 ± 1.9%) (Dunn's test, $P = 0.025$), while no difference was observed regarding calcite and aragonite crystals (KW test, $P = 0.258$ and $P = 0.148$, respectively) (Figure 2F). Focusing on aragonite crystals at the microstructure level, no significant difference in aragonite front spacing (Figure 2G and H) was measured on the pearl surface (KW test, $P = 0.950$), with a mean of 16.3 ± 1.9 µm in the control condition, 15.9 ± 1.7 µm in the 0.025 µg L^{-1} condition and 18.2 ± 3.9 µm in the 1 µg L^{-1} condition (Figure 2G). However, a significant difference in aragonite platelet thickness (Figure 2I and J) was measured (KW test, $P = 0.010$), with values of 491.9 ± 45.3, 442.4 ± 36.1 and 395.1 ± 18.5 nm in the control, 0.025 and 1 µg L^{-1} conditions, respectively, revealing a significantly lower value in the 1 µg L^{-1} condition compared to the control condition (Dunn's test, $P = 0.002$; Figure 2I).

Keshi pearl origin. Observation of keshi pearls under a stereomicroscope revealed the presence of a purple particle (~9 µm) embedded in the mineral surface microlayer of a keshi pearl (Figure 2K and L), displaying the characteristic color of weathered purple PE rope (Figure 2M and N). This superficial detection was uniquely observed in one keshi pearl produced from a pearl oyster exposed to 1 µg L^{-1} MNPs. The developed methodology did not enable the analysis and detection of a PE signature in this purple particle. Further details regarding the analysis of keshi pearls are presented in the Supporting Information.

RNA-Seq data. RNA sequencing of mantle ($N = 29$), hemocyte ($N = 29$), and pearl sac ($N = 29$) samples yielded means of 36.6 ± 4.5, 33.2 ± 3.3, and 34.4 ± 2.3 M raw reads per individual, respectively. After trimming, 95.2% of reads were recovered in mantle, hemocyte, and pearl sac samples and used for downstream analyses. The mapping rate reached 46.0 ± 1.1%, 36.1 ± 0.8%

and 42.2 ± 1.0% in mantle, hemocyte, and pearl sac samples, respectively, with no significant differences among conditions (ANOVA, $P = 0.609$, $P = 0.149$, and $P = 0.191$, respectively). Sequencing results and read survival after trimming and mapping are shown in Table S1.

Global gene expression patterns across tissues and conditions. The global sequencing results and retained reads were similar across conditions and tissues, as shown in Table S1. First, a hierarchical clustering analysis comparing the change in magnitude and direction of gene expression within each KOG class among datasets revealed that the patterns of the 0.025 and 1 µg L^{-1} conditions were mostly similar but tissue specific (Figure 3A–C). Indeed, *P. margaritifera* KOG functional enrichment correlated across conditions and tissues, with Pearson's r values of 0.74 ($P < 0.001$), 0.90 ($P < 0.001$) and 0.56 ($P = 0.004$) for the mantle, hemocytes and pearl sac, respectively (Figure 3A–C). No significant correlations in gene expression were detected among tissue samples from each MNP condition, except between mantle and pearl sac datasets for the 1 µg L^{-1} condition ($r = 0.59$, $P = 0.002$) (Figure S3).

In the mantle, individuals exposed to MNPs exhibited upregulation of genes involved in "energy production and conversion" (0.025 and 1 µg L^{-1}, $P_{adj} < 0.001$), which was the most significant enrichment, followed by "replication, recombination and repair" (0.025 µg L^{-1} MNPs, $P_{adj} = 0.049$; 1 µg L^{-1} MNPs, $P_{adj} = 0.016$). Regarding downregulated genes, the most significant enrichment common to both MNP conditions was associated with "cytoskeleton" (0.025 and 1 µg L^{-1}, $P_{adj} < 0.001$), although this KOG class was upregulated in hemocyte samples, followed by "signal transduction mechanisms" (0.025 and 1 µg L^{-1} MNPs, $P_{adj} < 0.001$, respectively) (Figure 3D). Hemocytes of exposed oysters also exhibited downregulation of genes associated with "nuclear structure" (0.025 µg L^{-1} MNPs, $P_{adj} = 0.047$; 1 µg L^{-1} MNPs, $P_{adj} < 0.001$), "RNA processing and modification" and "translation, ribosomal structure and biogenesis" (0.025 and 1 µg L^{-1} MNPs, $P_{adj} < 0.001$, respectively) (Figure 3D). Finally, in the pearl sac, individuals exposed

to MNP conditions exhibited common enrichment of upregulated genes involved in "chromatin structure and dynamics" (0.025 µg L^{-1} MNPs, $P_{adj} = 0.009$; 1 µg L^{-1} MNPs, $P_{adj} = 0.031$) (Figure 3D). Some unique patterns specific to MNP conditions were also observed, as shown in Figure 3D.

Gene coexpression modules associated with MNPs and physiological traits. The expression values of 23,610 genes in 29 mantle samples were used to construct the coexpression module by WGCNA. After clustering of module eigengenes (MEs) based on dissimilarity, a total of 10 modules (out of 26, Figure S4) were selected according to module-trait relationships ($r \geq 0.45$, $P \leq 0.01$) regarding correlations of ME expression with experimental conditions and physiological traits (Figures 4A and S5). Among the modules of interest, 5 modules were identified in cluster 1, 4 modules in cluster 2, and 1 module in cluster 3 (Figure 4A). The tan module (N = 718 genes; cluster 3) was identified as a key module showing a strong correlation with condition ($r = 0.67$, $P < 0.001$), specifically with 1 µg L^{-1} MNPs ($r = 0.69$, $P < 0.001$), and strong correlations with physiological traits such as ingestion ($r = 0.54$, $P = 0.002$) and assimilation ($r = –0.45$, $P = 0.01$) (Figure 4A). This module exhibited significantly higher ME expression in the 1 µg L^{-1} group than in both the control and 0.025 µg L^{-1} groups (Dunn's test, $P = 0.007$ and $P = 0.014$, respectively) (Figure 4B). The tan module was significantly enriched for "MAPK cascade", "omega-hydroxylase P450 pathway", "response to potassium ion" and "inorganic anion transport" (Figure 4C). Additional information regarding ME expression across the modules of interest and representative GO enrichments for modules displaying significant differences between conditions can be found in Figure 4B and C, as well as in the Supporting Information as Supplementary Results. Comprehensive details concerning all GO enrichments in BP and MF for the modules of interest are provided in Table S2.

Regarding the DEGs between the MNP conditions and the control conditions, a total of 438 DEGs were identified, with 88 DEGs *vs.* 0.025 µg L^{-1} MNPs and 405 DEGs *vs.* 1 µg L^{-1} MNPs;

of these DEGs, 55 were common to both MNP conditions (Figure 4D). A total of 24 and 64 up- and downregulated genes were found, respectively, from individuals treated under the 0.025 µg L^{-1} condition compared with the control and 246 and 159 up- and downregulated genes, respectively, from individuals treated under the 1 µg L^{-1} condition (Figure S6). Focusing on the tan module, a total of 82 DEGs (7 and 82 DEGs from 0.025 and 1 µg L^{-1} MNPs, respectively) were identified among the module genes, with 53 genes annotated according to UniProt entries (Table S4). All DEGs were upregulated, and 7 DEGs were common to both MNP conditions, of which 6 were annotated (Figure 4E and Table S4). Furthermore, by focusing on shared DEGs among sample types ($N = 5$ DEGs; Figure S7), a total of 4 DEGs were identified in the tan module (Figure 4E and Table S4), namely, *CYP2C8, CYP2J2* (cytochrome P450 transcripts), *HR4* (hormone receptor 4), and *SULT1B1* (sulfotransferase family 1B member 1), as being specific to the 1 µg L^{-1} condition (Figure S7). A complete list of DEG distribution among WGCNA modules in mantle samples is available in Table S3.

The WGCNA approach did not identify a module of interest with biomineralization-related genes in pearl sac samples, as no significant correlation was observed between conditions and pearl quality traits. Supplementary Results concerning WGCNA, DEGs analysis and GO enrichment in hemocyte (Figure S6 and S8–S9, and Table S4–S5) and pearl sac (Figure S6 and S10, and Table S6) samples are presented in the Supporting Information.

Discussion

Biochemical and physiological processes involved in the life cycle of heterotrophic organisms are closely dependent on (*i*) their ability to extract essential energy from their environment through food intake and (*ii*) the orchestration of energy management across various levels of biological

organization. The findings of this study reveal that experimental exposure to MNPs, aligned with *in situ* MP mass concentrations, alters pearl oyster energy metabolism, resulting in consequences across individual, cellular, and molecular levels, along with disruption of the harvest and impairment of pearl quality traits.

The SFG defines the energy needed for growth beyond maintenance, serving as an indicator of an individual's potential to thrive in their environment. The SFG is primarily influenced by ingestion and assimilation efficiency,[43] which impact energy gain in bivalves.[44] Here, the linear decrease in assimilation efficiency observed in individuals exposed to MNPs at a notably lower level of 1 μg L^{-1} indicates that the presence of MNPs altered microalgae assimilation for an equal water volume filtered by oysters. However, the highest MNP concentration triggered compensatory behavior, traduced by higher ingestion rates, in pearl oysters. Similar increases in food intake to counter energetic loss were previously observed in the Pacific oyster after a 2-month exposure to micro-PS.[8] Energy gain through compensatory behavior, however, is constrained by a lower assimilation rate at higher MNPs exposure, ultimately influencing the final SFG. A disbalanced energy budget without compensatory behavior results in lower reserve energy contents in oysters exposed to 0.025 μg L^{-1} MNPs compared to the control condition (–3.5 μg mg^{-1}) and 1 μg L^{-1} MNPs (–3.3 μg mg^{-1}). Early glycogen depletion is consistent with its role as a rapidly mobilizable metabolic fuel to meet bivalves' sudden energy demands.[45] How recurrent mobilization of reserves without physiological compensation might lead to long-term detrimental effects on individual's fitness remains to be determined.[46]

Molecular approaches employing dose-increasing exposure reveal tissue-specific responses that are largely conserved across MNPs concentrations but may diverge in terms of response intensity. Notably, the mantle's upregulated genes related to "energy production and conversion" highlight a hypothesized bioenergetic response to protect cells from oxidative stress.[47] Highest

MNPs concentration only triggers mitogen-activated protein kinase (MAPK) cascade together with stress response mechanisms, encompassing the response to potassium ions and the ω-hydroxylase P450 pathway. MAPK pathways (p38, JNK, and ERK) relay signals from various stimuli, triggering physiological responses including proliferation, differentiation, development, inflammation, stress, and apoptosis.[48] MAPK activation is linked to reactive oxygen species (ROS) production in micro-PS-exposed marine copepods.[49] Activation of potassium channels, linked to ATP hydrolysis for energy production, is proposed as an early oxidative stress response.[50] Meanwhile, cytochrome P450 ω-hydroxylases play a vital role in xenobiotic detoxification and lipid metabolism.[51] Indeed, MPs are known to reduce lipid digestion by forming large lipid-MP heteroaggregates and reducing lipase activity.[52] Conversely, moderated exposure also reveals unique gene signature enrichments in pairwise differential expression analysis, such as "carbohydrate transport and metabolism", observed in oysters exposed at 0.025 µg L^{-1}. This enrichment is key to understanding the observed low glycogen levels in oyster muscle. A depletion of cellular energy stores (carbohydrates, lipids and proteins) has previously been demonstrated in mussels exposed to micro-PS.[45] Convergent signals both biochemical on the glycogen content and molecular on the expression levels of genes involved in the metabolism of glycogen and wholly carbohydrates constitute a strong element of support for this energy hypothesis. This immediate stress response likely precedes the suggested secondary cellular homeostasis response in the 1 µg L^{-1} condition, engaging a plethora of genes that restore equilibrium under new environmental regime.[53] This distinction is accentuated by the notable disparity in the total number of DEGs, which were nearly five times more abundant in the mantle of individuals exposed to 1 µg L^{-1} MNPs (N = 405) compared to those exposed to 0.025 µg L^{-1} MNPs (N = 88). This reinforces the concept of a dose-specific transcriptomic disruption in energy metabolism, as previously suggested.[25] The physiological and molecular signs seen in pearl oysters exposed to both MNP conditions indicate

hallmarks of "*pejus*" conditions, characterized by reduced fitness but positive growth and reproduction.[46] However, the more pronounced molecular disorders observed in the 1 µg L^{-1} condition appear to reflect *P. margaritifera*'s gradual transition from "*pejus*" to "*pessimum*" conditions, representing a high degree of stress.[46] Notably, certain distinct patterns, such as "secondary metabolite biosynthesis, transport, and catabolism", enriched among upregulated genes in the 1 µg L^{-1} condition, may illustrate an energy metabolism shift linked to defense mechanisms. Secondary metabolites (SMs) are typically produced to serve crucial roles in an organism's interaction with its environment. These modifications of central metabolite precursors (*e.g.*, carbohydrates, lipids, and amino acids) enhance acclimation to environmental constraints.[54] While some animal SMs originate internally, most are diet-derived,[55] often through plant consumption.[56] Ingested SMs, whether directly or *via* MPs following adsorption,[57] can influence metabolic rates, nutrient digestibility, and energy expenditure based on type and quantity.[58] Moreover, animals exploit SMs as a strategy to counter challenges that disturb homeostasis due to their bioactive attributes, like antioxidants countering oxidative damage.[58] Further investigation is essential to comprehend SM origins and their role in *P. margaritifera* homeostasis. This requires consideration of interactions between microalgae-derived chemicals and MNPs, which could significantly explain both direct and indirect MNP effects on the environment and biodiversity.

Pearl quality assessment revealed significant effects of MNP exposure on pearl nacre microstructure, particularly impacting aragonite crystals and resulting in thinner aragonite platelets at 1 µg L^{-1} MNPs. Interestingly, depositing thick aragonite crystal layers early in the culturing process, followed by thinner layers near the pearl's surface in the later phase before harvest, could be advantageous for luster and color.[59] However, this effect was observed early, after a 3-month experimental cycle under MNP exposure. In contrast, natural pearl production spans over 18 months, raising questions about the long-term effects of MNPs on pearl quality. This is particularly

noteworthy as Japanese farmers harvest pearls in December, when water temperatures approach the upper limits of tolerance for oysters, since low temperatures induce a reduction in platelet thickness and pearl growth in *P. fucata*.[60] This outcome suggests that the thinner aragonite platelets observed in the present study at 1 µg L^{-1} MNPs may result from the energy metabolism disorder,[61,62] and that the presence of MNPs in pearl farming lagoons could potentially lead to the production of lower-quality pearls without lengthening the production cycle. Additionally, the harvest conducted after experimental exposure revealed that pearl oysters, which had rejected their nucleus post-grafting, yielded significantly more keshi pearls at 1 µg L^{-1} than oysters in the control condition exhibiting no keshi pearl. It's therefore possible that MNPs triggered keshi pearl production through the potential translocation of MNPs across epithelial membranes,[63] and/or external MNP intrusion *via* the incision created on the pearl pouch by the operator before receiver oyster healing. Indeed, small plastic particles can be embedded into shells during biomineralization.[64] While PE-PP particles were not detected within the mineral matrix of keshi pearls, microscopy revealed a particle with the expected size, shape, and color—a distinct purple akin to the purple PE rope used for MNP production and exposure. Despite the occasional value represented by keshi pearls, the presence of MNPs in the pearl pouch could potentially interfere with the biomineralization processes of pearl production, warranting further research.

In conclusion, this study demonstrated that mimicking the *in situ* conditions of MNP exposure can adversely influence various facets of energy metabolism in *P. margaritifera*. This interference affects energy assimilation, conversion, and increases energy costs for basal maintenance.[46] At a concentration of 1 µg L^{-1} MNPs, a compensatory effect on food intake was observed, potentially balancing the reduced energy intake due to digestive disruptions in molecular functions related to lipid metabolism. No such mechanism was seen at 0.025 µg L^{-1} MNPs, thus explaining the energy budget. It's important to note that stronger impacts might emerge at lower

doses, a significant consideration for comprehending plastic pollution effects on ecosystems. Stress is exacerbated by food availability.[65] Given the oligotrophic nature of lagoon ecosystems, far from the nonlimiting food supply we applied experimentally, stronger effects could arise under natural conditions. This is especially pertinent considering the presence of multiple stressors, such as temperature and acidification linked to global change, which could profoundly impact marine organisms when combined with MNP exposure.[66] This study underscores the risk posed by MNPs within the environmental exposure spectrum (exposome) confronting pearl oysters, their related economy, and lagoon ecosystems in French Polynesia.

Associated content

Supporting Information

The Supporting Information is available in attached file.

Supplementary Methods and Results encompassing ecophysiological and functional parameters, along with transcriptomic approaches. Supplementary Figures (S1 to S10) and Tables (S1 to S6) including details about polymer identification of MNP, particle size distribution, and RNA-Seq data analysis (PDF).

Data Availability

RNA-Seq data were deposited into the European Bioinformatics Institute–European Nucleotide Archive (EBI–ENA) databank under the project ID PRJEB63073. Additional data are presented in the main text of this article and the Supporting Information file.

Author information

Author Contributions

T.G., G.L.M., and A.H. designed and supervised the research. T.G., J.L.L., C.S., F.L., and A.D. conducted the research. T.G. and J.L.L. analyzed the data. T.G. visualized the data and drafted the original manuscript, which was reviewed by J.L.L., A.D., I.P.P., and A.H., and edited by T.G. All authors discussed the data and approved the manuscript.

Notes

The authors declare no competing financial interest.

Acknowledgments

The authors thank L. Bish from Ifremer for providing microalgae throughout the 5-month experiment. Appreciation is also expressed to G. Duflos, C. Himber and M. Colin from Anses, M. Kazour from the LOG and K. Mahé from Ifremer for participation in keshi pearl analyses. The Ifremer Bioinformatics Core Facility (SeBiMER; https://ifremer-bioinformatics.github.io/) receives acknowledgment for providing technical help and scientific support for bioinformatics analysis. We extend our gratitude to the *Pôle de Calcul et de Données Marines* (PCDM; https://wwz.ifremer.fr/en/Research-Technology/Research-Infrastructures/Digital-infrastructures/Computation-Centre) for providing computing support and storage resources through DATARMOR.

The present study was supported by the MICROLAG project funded by the French Polynesian government under *Direction des Ressources Marines* (to T.G.), by a doctoral research grant No. 09793 from Ifremer (to T.G.), and by the European Union, the European Regional Development Fund (ERDF), the French State, the French Region Hauts-de-France and Ifremer under the framework of the project CPER MARCO 2015–2020 (to A.D.).

References

(1) Lebreton, L.; Andrady, A. Future Scenarios of Global Plastic Waste Generation and Disposal. *Palgrave Commun.* **2019**, *5* (1), 1–11. https://doi.org/10.1057/s41599-018-0212-7.

(2) Thompson, R. C. Lost at Sea: Where Is All the Plastic? *Science* **2004**, *304* (5672), 838–838. https://doi.org/10.1126/science.1094559.

(3) Andrady, A. L. Microplastics in the Marine Environment. *Mar. Pollut. Bull.* **2011**, *62* (8), 1596–1605. https://doi.org/10.1016/j.marpolbul.2011.05.030.

(4) Eriksen, M.; Lebreton, L. C. M.; Carson, H. S.; Thiel, M.; Moore, C. J.; Borerro, J. C.; Galgani, F.; Ryan, P. G.; Reisser, J. Plastic Pollution in the World's Oceans: More than 5 Trillion Plastic Pieces Weighing over 250,000 Tons Afloat at Sea. *PLoS ONE* **2014**, *9* (12), e111913. https://doi.org/10.1371/journal.pone.0111913.

(5) Schwaferts, C.; Niessner, R.; Elsner, M.; Ivleva, N. P. Methods for the Analysis of Submicrometer- and Nanoplastic Particles in the Environment. *TrAC Trends Anal. Chem.* **2019**, *112*, 52–65. https://doi.org/10.1016/j.trac.2018.12.014.

(6) Rochman, C. M.; Browne, M. A.; Underwood, A. J.; van Franeker, J. A.; Thompson, R. C.; Amaral-Zettler, L. A. The Ecological Impacts of Marine Debris: Unraveling the Demonstrated Evidence from What Is Perceived. *Ecology* **2016**, *97* (2), 302–312. https://doi.org/10.1890/14-2070.1.

(7) Galloway, T. S.; Cole, M.; Lewis, C. Interactions of Microplastic Debris throughout the Marine Ecosystem. *Nat. Ecol. Evol.* **2017**, *1* (5), 0116. https://doi.org/10.1038/s41559-017-0116.

(8) Sussarellu, R.; Suquet, M.; Thomas, Y.; Lambert, C.; Fabioux, C.; Pernet, M. E. J.; Le Goïc, N.; Quillien, V.; Mingant, C.; Epelboin, Y.; Corporeau, C.; Guyomarch, J.; Robbens, J.; Paul-Pont, I.; Soudant, P.; Huvet, A. Oyster Reproduction Is Affected by Exposure to Polystyrene Microplastics. *Proc. Natl. Acad. Sci.* **2016**, *113* (9), 2430–2435. https://doi.org/10.1073/pnas.1519019113.

(9) Gardon, T.; Reisser, C.; Soyez, C.; Quillien, V.; Le Moullac, G. Microplastics Affect Energy Balance and Gametogenesis in the Pearl Oyster *Pinctada Margaritifera*. *Environ. Sci. Technol.* **2018**, *52* (9), 5277–5286. https://doi.org/10.1021/acs.est.8b00168.

(10) Leslie, H. A.; Brandsma, S. H.; van Velzen, M. J. M.; Vethaak, A. D. Microplastics En Route: Field Measurements in the Dutch River Delta and Amsterdam Canals, Wastewater Treatment Plants, North Sea Sediments and Biota. *Environ. Int.* **2017**, *101*, 133–142. https://doi.org/10.1016/j.envint.2017.01.018.

(11) Bessa, F.; Barría, P.; Neto, J. M.; Frias, J. P. G. L.; Otero, V.; Sobral, P.; Marques, J. C. Occurrence of Microplastics in Commercial Fish from a Natural Estuarine Environment. *Mar. Pollut. Bull.* **2018**, *128*, 575–584. https://doi.org/10.1016/j.marpolbul.2018.01.044.

(12) Watts, A. J. R.; Urbina, M. A.; Goodhead, R.; Moger, J.; Lewis, C.; Galloway, T. S. Effect of Microplastic on the Gills of the Shore Crab *Carcinus Maenas*. *Environ. Sci. Technol.* **2016**, *50* (10), 5364–5369. https://doi.org/10.1021/acs.est.6b01187.

(13) Cole, M.; Lindeque, P.; Fileman, E.; Halsband, C.; Galloway, T. S. The Impact of Polystyrene Microplastics on Feeding, Function and Fecundity in the Marine Copepod *Calanus Helgolandicus*. *Environ. Sci. Technol.* **2015**, *49* (2), 1130–1137. https://doi.org/10.1021/es504525u.

(14) Watts, A. J. R.; Urbina, M. A.; Corr, S.; Lewis, C.; Galloway, T. S. Ingestion of Plastic Microfibers by the Crab *Carcinus Maenas* and Its Effect on Food Consumption and Energy Balance. *Environ. Sci. Technol.* **2015**, *49* (24), 14597–14604. https://doi.org/10.1021/acs.est.5b04026.

(15) Phuong, N. N.; Zalouk-Vergnoux, A.; Poirier, L.; Kamari, A.; Châtel, A.; Mouneyrac, C.; Lagarde, F. Is There Any Consistency between the Microplastics Found in the Field and Those Used in Laboratory Experiments? *Environ. Pollut.* **2016**, *211*, 111–123. https://doi.org/10.1016/j.envpol.2015.12.035.

(16) Lenz, R.; Enders, K.; Nielsen, T. G. Microplastic Exposure Studies Should Be Environmentally Realistic. *Proc. Natl. Acad. Sci.* **2016**, *113* (29), E4121–E4122. https://doi.org/10.1073/pnas.1606615113.

(17) Paul-Pont, I.; Tallec, K.; Gonzalez-Fernandez, C.; Lambert, C.; Vincent, D.; Mazurais, D.; Zambonino-Infante, J.-L.; Brotons, G.; Lagarde, F.; Fabioux, C.; Soudant, P.; Huvet, A. Constraints and Priorities for Conducting Experimental Exposures of Marine Organisms to Microplastics. *Front. Mar. Sci.* **2018**, *5*, 252. https://doi.org/10.3389/fmars.2018.00252.

(18) Revel, M.; Lagarde, F.; Perrein-Ettajani, H.; Bruneau, M.; Akcha, F.; Sussarellu, R.; Rouxel, J.; Costil, K.; Decottignies, P.; Cognie, B.; Châtel, A.; Mouneyrac, C. Tissue-Specific Biomarker Responses in the Blue Mussel *Mytilus* Spp. Exposed to a Mixture of Microplastics at Environmentally Relevant Concentrations. *Front. Environ. Sci.* **2019**, *7*, 33. https://doi.org/10.3389/fenvs.2019.00033.

(19) Pannetier, P.; Morin, B.; Le Bihanic, F.; Dubreil, L.; Clérandeau, C.; Chouvellon, F.; Van Arkel, K.; Danion, M.; Cachot, J. Environmental Samples of Microplastics Induce Significant Toxic Effects in Fish Larvae. *Environ. Int.* **2020**, *134*, 105047. https://doi.org/10.1016/j.envint.2019.105047.
(20) Schür, C.; Zipp, S.; Thalau, T.; Wagner, M. Microplastics but Not Natural Particles Induce Multigenerational Effects in *Daphnia Magna*. *Environ. Pollut.* **2020**, *260*, 113904. https://doi.org/10.1016/j.envpol.2019.113904.
(21) Koelmans, A. A.; Besseling, E.; Foekema, E.; Kooi, M.; Mintenig, S.; Ossendorp, B. C.; Redondo-Hasselerharm, P. E.; Verschoor, A.; van Wezel, A. P.; Scheffer, M. Risks of Plastic Debris: Unravelling Fact, Opinion, Perception, and Belief. *Environ. Sci. Technol.* **2017**, *51* (20), 11513–11519. https://doi.org/10.1021/acs.est.7b02219.
(22) Siu, D. Les exportations de produits perliers, fortement impactées par la Covid-19 en 2020. *Inst. Stat. Polynésie Fr.* **2021**, No. 1274, 4.
(23) Andréfouët, S.; Thomas, Y.; Lo, C. Amount and Type of Derelict Gear from the Declining Black Pearl Oyster Aquaculture in Ahe Atoll Lagoon, French Polynesia. *Mar. Pollut. Bull.* **2014**, *83* (1), 224–230. https://doi.org/10.1016/j.marpolbul.2014.03.048.
(24) Gardon, T.; El Rakwe, M.; Paul-Pont, I.; Le Luyer, J.; Thomas, L.; Prado, E.; Boukerma, K.; Cassone, A.-L.; Quillien, V.; Soyez, C.; Costes, L.; Crusot, M.; Dreanno, C.; Le Moullac, G.; Huvet, A. Microplastics Contamination in Pearl-Farming Lagoons of French Polynesia. *J. Hazard. Mater.* **2021**, *419*, 126396. https://doi.org/10.1016/j.jhazmat.2021.126396.
(25) Gardon, T.; Morvan, L.; Huvet, A.; Quillien, V.; Soyez, C.; Le Moullac, G.; Le Luyer, J. Microplastics Induce Dose-Specific Transcriptomic Disruptions in Energy Metabolism and Immunity of the Pearl Oyster *Pinctada Margaritifera*. *Environ. Pollut.* **2020**, *266*, 115180. https://doi.org/10.1016/j.envpol.2020.115180.
(26) Gardon, T.; Paul-Pont, I.; Le Moullac, G.; Soyez, C.; Lagarde, F.; Huvet, A. Cryogrinding and Sieving Techniques as Challenges towards Producing Controlled Size Range Microplastics for Relevant Ecotoxicological Tests. *Environ. Pollut.* **2022**, *315*, 120383. https://doi.org/10.1016/j.envpol.2022.120383.
(27) Pouvreau, S.; Jonquières, G.; Buestel, D. Filtration by the Pearl Oyster, *Pinctada Margaritifera*, under Conditions of Low Seston Load and Small Particle Size in a Tropical Lagoon Habitat. *Aquaculture* **1999**, *176* (3–4), 295–314. https://doi.org/10.1016/S0044-8486(99)00102-7.
(28) Vahirua-Lechat, I.; Laure, F.; LeCoz, J. R.; Bianchini, J. P.; Bellais, M.; Le Moullac, G. Changes in Fatty Acid and Sterol Composition during Oogenesis in the Pearl Oyster *Pinctada Margaritifera*. *Aquac. Res.* **2008**, *39* (16), 1739–1746. https://doi.org/10.1111/j.1365-2109.2008.02050.x.
(29) Linard, C.; Gueguen, Y.; Moriceau, J.; Soyez, C.; Hui, B.; Raoux, A.; Cuif, J. P.; Cochard, J.-C.; Le Pennec, M.; Le Moullac, G. Calcein Staining of Calcified Structures in Pearl Oyster *Pinctada Margaritifera* and the Effect of Food Resource Level on Shell Growth. *Aquaculture* **2011**, *313* (1), 149–155. https://doi.org/10.1016/j.aquaculture.2011.01.008.
(30) Khosrovyan, A.; Kahru, A. Virgin and UV-Weathered Polyamide Microplastics Posed No Effect on the Survival and Reproduction of *Daphnia Magna*. *PeerJ* **2022**, *10*, e13533. https://doi.org/10.7717/peerj.13533.
(31) Gueguen, Y.; Czorlich, Y.; Mastail, M.; Le Tohic, B.; Defay, D.; Lyonnard, P.; Marigliano, D.; Gauthier, J.-P.; Bari, H.; Lo, C.; Chabrier, S.; Le Moullac, G. Yes, It Turns: Experimental Evidence of Pearl Rotation during Its Formation. *R. Soc. Open Sci.* **2015**, *2* (7), 150144. https://doi.org/10.1098/rsos.150144.
(32) Le Moullac, G.; Schuck, L.; Chabrier, S.; Belliard, C.; Lyonnard, P.; Broustal, F.; Soyez, C.; Saulnier, D.; Brahmi, C.; Ky, C.-L.; Beliaeff, B. Influence of Temperature and Pearl Rotation on Biomineralization in the Pearl Oyster, *Pinctada Margaritifera*. *J. Exp. Biol.* **2018**, *221* (18), jeb186858. https://doi.org/10.1242/jeb.186858.
(33) Chávez-Villalba, J.; Soyez, C.; Aurentz, H.; Le Moullac, G. Physiological Responses of Female and Male Black-Lip Pearl Oysters *(Pinctada Margaritifera)* to Different Temperatures and Concentrations of Food. *Aquat. Living Resour.* **2013**, *26* (3), 263–271. https://doi.org/10.1051/alr/2013059.
(34) Hermabessiere, L.; Himber, C.; Boricaud, B.; Kazour, M.; Amara, R.; Cassone, A.-L.; Laurentie, M.; Paul-Pont, I.; Soudant, P.; Dehaut, A.; Duflos, G. Optimization, Performance, and Application of a Pyrolysis-GC/MS Method for the Identification of Microplastics. *Anal. Bioanal. Chem.* **2018**, *410* (25), 6663–6676. https://doi.org/10.1007/s00216-018-1279-0.
(35) Djouina, M.; Vignal, C.; Dehaut, A.; Caboche, S.; Hirt, N.; Waxin, C.; Himber, C.; Beury, D.; Hot, D.; Dubuquoy, L.; Launay, D.; Duflos, G.; Body-Malapel, M. Oral Exposure to Polyethylene Microplastics Alters Gut Morphology, Immune Response, and Microbiota Composition in Mice. *Environ. Res.* **2022**, *212*, 113230. https://doi.org/10.1016/j.envres.2022.113230.
(36) Bolger, A. M.; Lohse, M.; Usadel, B. Trimmomatic: A Flexible Trimmer for Illumina Sequence Data. *Bioinformatics* **2014**, *30* (15), 2114–2120. https://doi.org/10.1093/bioinformatics/btu170.

(37) Ewels, P.; Magnusson, M.; Lundin, S.; Käller, M. MultiQC: Summarize Analysis Results for Multiple Tools and Samples in a Single Report. *Bioinformatics* **2016**, *32* (19), 3047–3048. https://doi.org/10.1093/bioinformatics/btw354.
(38) Le Luyer, J.; Auffret, P.; Quillien, V.; Leclerc, N.; Reisser, C.; Vidal-Dupiol, J.; Ky, C.-L. Whole Transcriptome Sequencing and Biomineralization Gene Architecture Associated with Cultured Pearl Quality Traits in the Pearl Oyster, *Pinctada Margaritifera*. *BMC Genomics* **2019**, *20* (1), 111. https://doi.org/10.1186/s12864-019-5443-5.
(39) Wu, T. D.; Reeder, J.; Lawrence, M.; Becker, G.; Brauer, M. J. GMAP and GSNAP for Genomic Sequence Alignment: Enhancements to Speed, Accuracy, and Functionality. In *Statistical Genomics: Methods and Protocols*; Mathé, E., Davis, S., Eds.; Methods in Molecular Biology; Springer New York: New York, NY, 2016; pp 283–334. https://doi.org/10.1007/978-1-4939-3578-9_15.
(40) Love, M. I.; Huber, W.; Anders, S. Moderated Estimation of Fold Change and Dispersion for RNA-Seq Data with DESeq2. *Genome Biol.* **2014**, *15* (12), 550. https://doi.org/10.1186/s13059-014-0550-8.
(41) Dixon, G. B.; Davies, S. W.; Aglyamova, G. V.; Meyer, E.; Bay, L. K.; Matz, M. V. Genomic Determinants of Coral Heat Tolerance across Latitudes. *Science* **2015**, *348* (6242), 1460–1462. https://doi.org/10.1126/science.1261224.
(42) Huerta-Cepas, J.; Forslund, K.; Coelho, L. P.; Szklarczyk, D.; Jensen, L. J.; von Mering, C.; Bork, P. Fast Genome-Wide Functional Annotation through Orthology Assignment by eggNOG-Mapper. *Mol. Biol. Evol.* **2017**, *34* (8), 2115–2122. https://doi.org/10.1093/molbev/msx148.
(43) Albentosa, M.; Viñas, L.; Besada, V.; Franco, A.; González-Quijano, A. First Measurements of the Scope for Growth (SFG) in Mussels from a Large Scale Survey in the North-Atlantic Spanish Coast. *Sci. Total Environ.* **2012**, *435–436*, 430–445. https://doi.org/10.1016/j.scitotenv.2012.07.025.
(44) Hawkins, A.; James, M.; Hickman, R.; Hatton, S.; Weatherhead, M. Modelling of Suspension-Feeding and Growth in the Green-Lipped Mussel *Perna Canaliculus* Exposed to Natural and Experimental Variations of Seston Availability in the Marlborough Sounds, New Zealand. *Mar. Ecol. Prog. Ser.* **1999**, *191*, 217–232. https://doi.org/10.3354/meps191217.
(45) Shang, Y.; Wang, X.; Chang, X.; Sokolova, I. M.; Wei, S.; Liu, W.; Fang, J. K. H.; Hu, M.; Huang, W.; Wang, Y. The Effect of Microplastics on the Bioenergetics of the Mussel *Mytilus Coruscus* Assessed by Cellular Energy Allocation Approach. *Front. Mar. Sci.* **2021**, *8*, 754789. https://doi.org/10.3389/fmars.2021.754789.
(46) Sokolova, I. M. Energy-Limited Tolerance to Stress as a Conceptual Framework to Integrate the Effects of Multiple Stressors. *Integr. Comp. Biol.* **2013**, *53* (4), 597–608. https://doi.org/10.1093/icb/ict028.
(47) Crawford, D. R.; Wang, Y.; Schools, G. P.; Kochheiser, J.; Davies, K. J. Down-Regulation of Mammalian Mitochondrial RNAs during Oxidative Stress. *Free Radic. Biol. Med.* **1997**, *22* (3), 551–559. https://doi.org/10.1016/s0891-5849(96)00380-2.
(48) Zhang, W.; Liu, H. T. MAPK Signal Pathways in the Regulation of Cell Proliferation in Mammalian Cells. *Cell Res.* **2002**, *12* (1), 9–18. https://doi.org/10.1038/sj.cr.7290105.
(49) Jeong, C.-B.; Kang, H.-M.; Lee, M.-C.; Kim, D.-H.; Han, J.; Hwang, D.-S.; Souissi, S.; Lee, S.-J.; Shin, K.-H.; Park, H. G.; Lee, J.-S. Adverse Effects of Microplastics and Oxidative Stress-Induced MAPK/Nrf2 Pathway-Mediated Defense Mechanisms in the Marine Copepod *Paracyclopina Nana*. *Sci. Rep.* **2017**, *7* (41323). https://doi.org/10.1038/srep41323.
(50) Udensi, U. K.; Tchounwou, P. B. Potassium Homeostasis, Oxidative Stress, and Human Disease. *Int. J. Clin. Exp. Physiol.* **2017**, *4* (3), 111–122. https://doi.org/10.4103/ijcep.ijcep_43_17.
(51) Ni, K.-D.; Liu, J.-Y. The Functions of Cytochrome P450 ω-Hydroxylases and the Associated Eicosanoids in Inflammation-Related Diseases. *Front. Pharmacol.* **2021**, *12*, 716801. https://doi.org/10.3389/fphar.2021.716801.
(52) Tan, H.; Yue, T.; Xu, Y.; Zhao, J.; Xing, B. Microplastics Reduce Lipid Digestion in Simulated Human Gastrointestinal System. *Environ. Sci. Technol.* **2020**, *54* (19), 12285–12294. https://doi.org/10.1021/acs.est.0c02608.
(53) Kültz, D. Molecular and Evolutionary Basis of the Cellular Stress Response. *Annu. Rev. Physiol.* **2005**, *67*, 225–257. https://doi.org/10.1146/annurev.physiol.67.040403.103635.
(54) Pott, D. M.; Osorio, S.; Vallarino, J. G. From Central to Specialized Metabolism: An Overview of Some Secondary Compounds Derived From the Primary Metabolism for Their Role in Conferring Nutritional and Organoleptic Characteristics to Fruit. *Front. Plant Sci.* **2019**, *10*, 835. https://doi.org/10.3389/fpls.2019.00835.
(55) Torres, J. P.; Schmidt, E. W. The Biosynthetic Diversity of the Animal World. *J. Biol. Chem.* **2019**, *294* (46), 17684–17692. https://doi.org/10.1074/jbc.REV119.006130.

(56) Chomel, M.; Guittonny-Larchevêque, M.; Fernandez, C.; Gallet, C.; DesRochers, A.; Paré, D.; Jackson, B. G.; Baldy, V. Plant Secondary Metabolites: A Key Driver of Litter Decomposition and Soil Nutrient Cycling. *J. Ecol.* **2016**, *104* (6), 1527–1541. https://doi.org/10.1111/1365-2745.12644.
(57) Kim, S. W.; Liang, Y.; Lozano, Y. M.; Rillig, M. C. Microplastics Reduce the Negative Effects of Litter-Derived Plant Secondary Metabolites on Nematodes in Soil. *Front. Environ. Sci.* **2021**, *9*, 790560. https://doi.org/10.3389/fenvs.2021.790560.
(58) Forbey, J. S.; Harvey, A. L.; Huffman, M. A.; Provenza, F. D.; Sullivan, R.; Tasdemir, D. Exploitation of Secondary Metabolites by Animals: A Response to Homeostatic Challenges. *Integr. Comp. Biol.* **2009**, *49* (3), 314–328. https://doi.org/10.1093/icb/icp046.
(59) Muhammad, G.; Atsumi, T.; Sunardi; Komaru, A. Nacre Growth and Thickness of Akoya Pearls from Japanese and Hybrid *Pinctada Fucata* in Response to the Aquaculture Temperature Condition in Ago Bay, Japan. *Aquaculture* **2017**, *477*, 35–42. https://doi.org/10.1016/j.aquaculture.2017.04.032.
(60) Muhammad, G.; Atsumi, T.; Komaru, A. The Influence of Water Temperature, Salinity and Food Availability on Nacre Deposition Rates in Shells and Pearls of Japanese and Hybrid Pearl Oyster, *Pinctada Fucata* (Gould, 1850). *Aquaculture* **2020**, *528*, 735512. https://doi.org/10.1016/j.aquaculture.2020.735512.
(61) Joubert, C.; Linard, C.; Le Moullac, G.; Soyez, C.; Saulnier, D.; Teaniniuraitemoana, V.; Ky, C. L.; Gueguen, Y. Temperature and Food Influence Shell Growth and Mantle Gene Expression of Shell Matrix Proteins in the Pearl Oyster *Pinctada Margaritifera*. *PLoS ONE* **2014**, *9* (8), e103944. https://doi.org/10.1371/journal.pone.0103944.
(62) Le Pabic, L.; Parrad, S.; Sham Koua, M.; Nakasai, S.; Saulnier, D.; Devaux, D.; Ky, C.-L. Culture Site Dependence on Pearl Size Realization in *Pinctada Margaritifera* in Relation to Recipient Oyster Growth and Mantle Graft Biomineralization Gene Expression Using the Same Donor Phenotype. *Estuar. Coast. Shelf Sci.* **2016**, *182*, 294–303. https://doi.org/10.1016/j.ecss.2016.03.009.
(63) Al-Sid-Cheikh, M.; Rowland, S. J.; Stevenson, K.; Rouleau, C.; Henry, T. B.; Thompson, R. C. Uptake, Whole-Body Distribution, and Depuration of Nanoplastics by the Scallop *Pecten Maximus* at Environmentally Realistic Concentrations. *Environ. Sci. Technol.* **2018**, *52* (24), 14480–14486. https://doi.org/10.1021/acs.est.8b05266.
(64) Han, Z.; Jiang, T.; Xie, L.; Zhang, R. Microplastics Impact Shell and Pearl Biomineralization of the Pearl Oyster *Pinctada Fucata*. *Environ. Pollut.* **2021**, 118522. https://doi.org/10.1016/j.envpol.2021.118522.
(65) Cominassi, L.; Moyano, M.; Claireaux, G.; Howald, S.; Mark, F. C.; Zambonino-Infante, J.-L.; Peck, M. A. Food Availability Modulates the Combined Effects of Ocean Acidification and Warming on Fish Growth. *Sci. Rep.* **2020**, *10* (1), 2338. https://doi.org/10.1038/s41598-020-58846-2.
(66) Wen, B.; Zhang, N.; Jin, S.-R.; Chen, Z.-Z.; Gao, J.-Z.; Liu, Y.; Liu, H.-P.; Xu, Z. Microplastics Have a More Profound Impact than Elevated Temperatures on the Predatory Performance, Digestion and Energy Metabolism of an Amazonian Cichlid. *Aquat. Toxicol.* **2018**, *195*, 67–76. https://doi.org/10.1016/j.aquatox.2017.12.010.

Figures

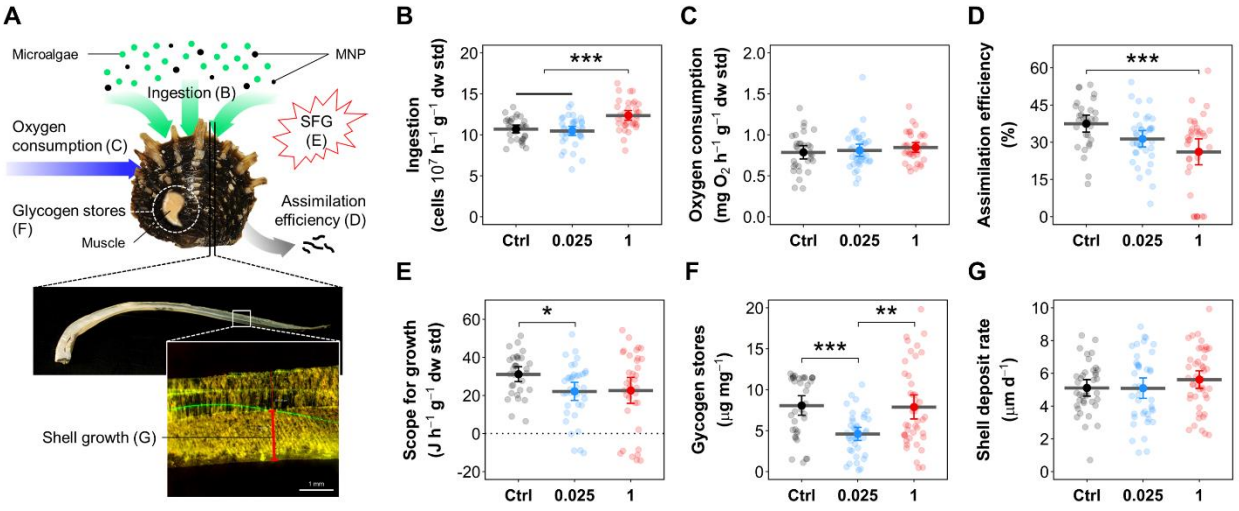

Figure 1. Physiological parameters of *P. margaritifera* exposed to micro-nanoplastics. (A) Schematic of the monitored ecophysiological parameters. (B to G) Boxplots showing the effect of MNP exposure on (B) ingestion rate, (C) oxygen consumption, (D) assimilation efficiency, (E) scope for growth (SFG), (F) glycogen stores and (G) shell growth. Data are expressed as the mean with the 95% confidence interval ($31 \leq N \leq 46$). Asterisks indicate statistically significant differences between conditions ("*", $P < 0.05$; "**", $P < 0.01$; "***", $P < 0.001$).

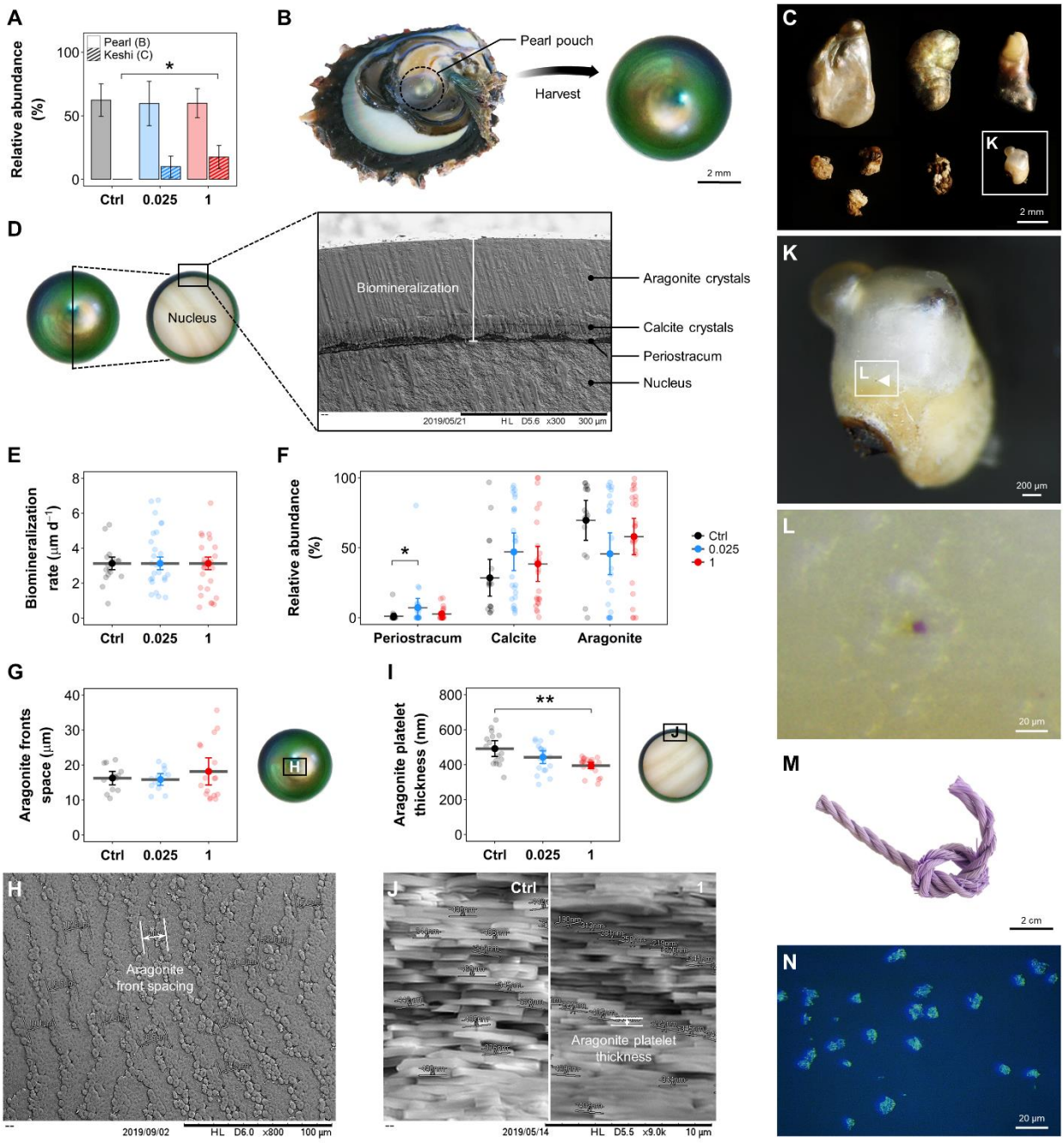

Figure 2. Functional results following a 3-month pearl production cycle under micro-nanoplastics exposure. (A) Histograms of the frequency distribution of collected (B) pearls and (C) keshi pearls showing different morphotypes. Pearl quality assessment was based on (D) biomineral secretion produced on the nucleus for 3 months, which was used to obtain (E) the biomineralization rate and

(F) the relative abundance of pearl nacre deposition structures composed of periostracum, calcite and aragonite crystals. The aragonite crystal microstructure was also characterized by measuring (G and H) the space between aragonite fronts on the pearl surface and (I and J) the platelet thickness on the pearl cross-section using SEM. (J) Two pooled SEM images illustrate comparison in aragonite platelet thickness between the control (left) and 1 MNP L^{-1} (right) conditions. (K and L) Observation of a particle with a purple color identified in the mineral surface microlayer of a keshi pearl. (M and N) Pictures of the weathered purple synthetic rope used to produce PE micro-nanoplastics in the present study. Data are expressed as the mean with the 95% confidence interval of the mean ($17 \leq N \leq 25$), except for A, which shows the mean ± standard deviation. Asterisks indicate statistically significant differences between conditions ("*", $P < 0.05$; "**", $P < 0.01$).

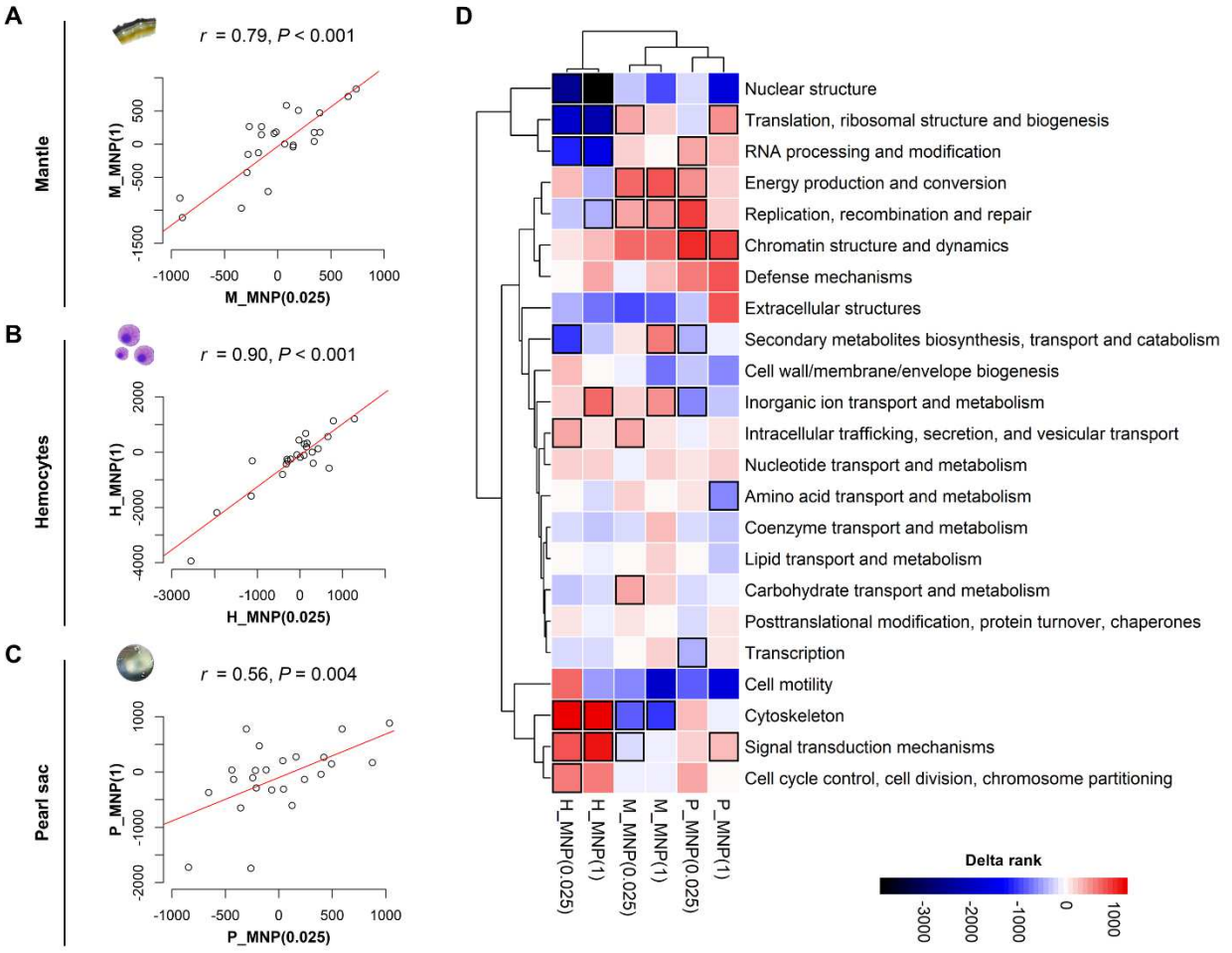

Figure 3. Hierarchical clustering analysis of KOG enrichments in the *P. margaritifera* transcriptome following micro-nanoplastics exposure. Pearson's correlations of KOG delta rank values in the (A) mantle, (B) hemocytes and (C) pearl sac of *P. margaritifera* exposed to 0.025 and 1 µg L^{-1} MNPs. (D) Shared KOG term enrichments (rows) among up- or downregulated genes (delta rank heatmap) under MNP conditions across tissues (columns; M: mantle, H: hemocytes or P: pearl sac). KOG categories in bolded squares denote statistically significant enrichments (FDR-adjusted $P < 0.05$).

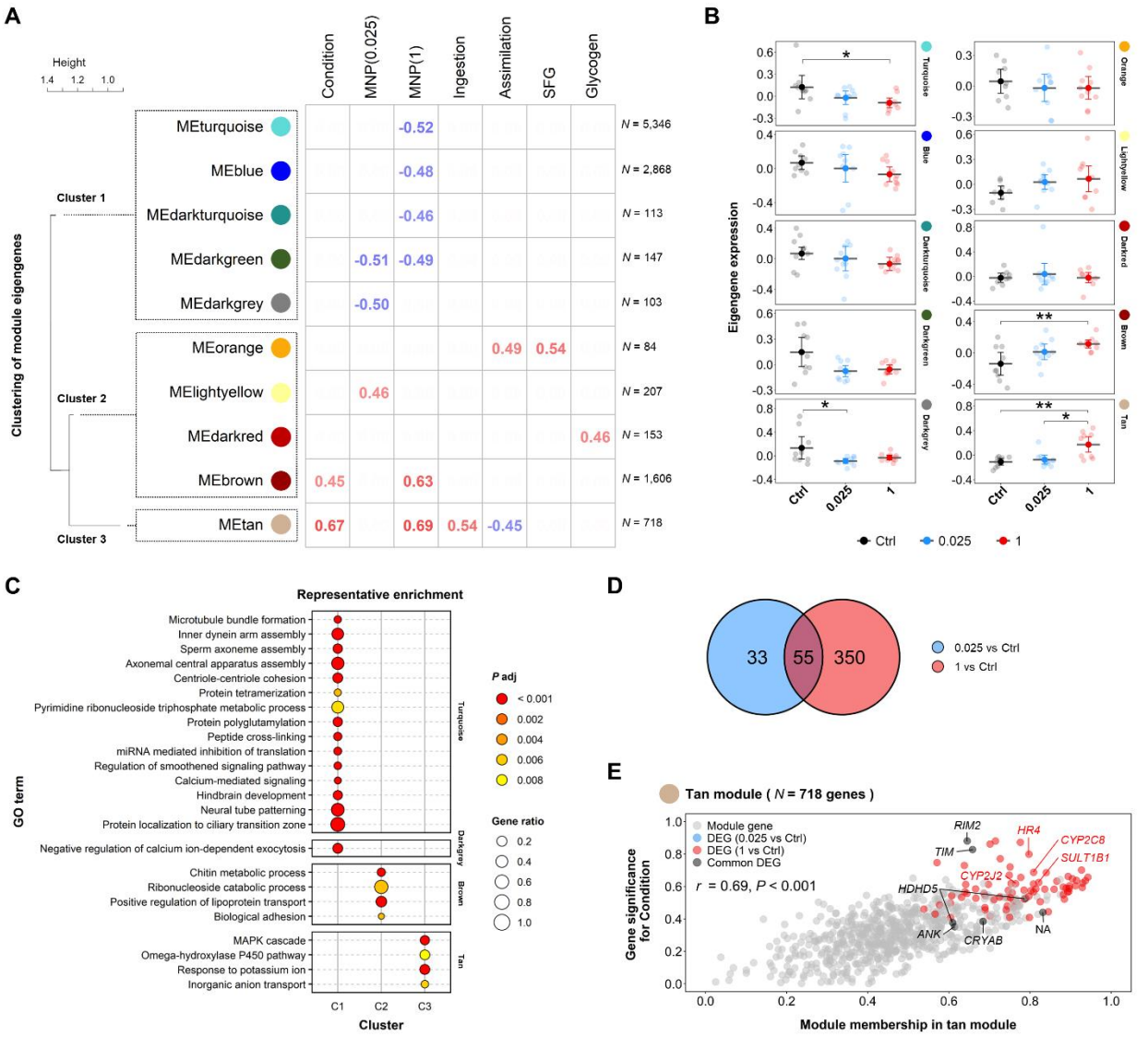

Figure 4. Transcriptomic responses in the mantle of *P. margaritifera* after a 5-month exposure to micro-nanoplastics. (A) Heatmap of identified modules (*y*-axis) and functionally enriched pathways in relation to experimental traits ($|r| \geq 0.45$, $P \leq 0.01$; *x*-axis) from WGCNA. The clustering tree of module eigengenes (MEs) on the left is based on a merging threshold of 100% dissimilarity initially established at 25% for network construction. The numbers on the right of the heatmap represent the number of genes identified in each module. (B) Eigengene expression for selected WGCNA modules significantly correlated with experimental conditions and/or

physiological traits in response to MNP exposure ("*", $P < 0.05$; "**", $P < 0.01$). Data are expressed as the mean with the 95% confidence interval ($N = 9–10$). (C) Representative functional enrichment analysis of module genes identified in the turquoise, darkgrey, brown and tan modules based on an adjusted *P*-value cutoff ($P < 0.01$) and cut-height (0.8) of the GO terms tree to obtain "independent groups". The dendrograms depict the sharing of genes between categories; the fractions correspond to genes with $P < 0.05$ relative to the total number of genes within the category. (D) Venn diagram of differentially expressed genes (DEGs) in both MNP conditions compared to the control ($|\log_2 FC| > 2$; FDR < 0.01). (E) Scatterplot of gene significance for condition *vs.* module membership in the tan module illustrating module-trait associations. Gray genes represent module genes; blue and red genes represent DEGs specific to 0.025 and 1 µg L^{-1} MNPs, respectively, with labeled red genes ($N = 4$) identified as common DEGs with other tissues (hemocytes and pearl sac) in the 1 µg L^{-1} condition, including *CYP2J2* and *CYP2C8* (cytochrome P450 family 2 subfamily J member 2 and subfamily C member 8, respectively), *HR4* (hormone receptor 4) and *SULT1B1* (sulfotransferase family 1B member 1); labeled black genes represent common DEGs in both MNP conditions ($N = 7$, of which 6 were annotated), including 2 transcript variants of *HDHD5* (haloacid dehalogenase-like hydrolase domain containing 5), *RIM2* (replication in mitochondria 2), *CRYAB* (crystallin alpha B), *TIM* (timeless) and *ANK* (ankyrin).

Supplementary Files

This is a list of supplementary files associated with this preprint. Click to download.

- Gardonetal2023SupportingInformation.pdf